ACCSCIENCE PUBLISHING

Eurasian Journal of Medicine and Oncology

ORIGINAL RESEARCH ARTICLE

Anticancer potential of flavonoids isolated from *Pistacia chinensis* against glioblastoma (U87) cell line: Extensive *in vitro* and *in silico* research

Abdur Rauf[1†*], Soonmin Ho[2], Muhammad Umer Khan[3], Iqra Khurram[3], Zuneera Akram[4], Yahya S. Al-Awthan[5,6], Omar S. Bahattab[5], and Marcello Iriti[7,8†*]

[1]Department of Chemistry, Faculty of Sciences, University of Swabi, Swabi, Khyber Pakhtunkhwa, Pakistan

[2]Faculty of Health and Life Sciences, INTI International University, Nilai, Negeri Sembilan, Malaysia

[3]Institute of Molecular Biology and Biotechnology, Faculty of Sciences, The University of Lahore, Lahore, Punjab, Pakistan

[4]Department of Pharmacology, Faculty of Pharmaceutical Sciences, Baqai Medical University, Karachi, Sindh, Pakistan

[5]Department of Biology, Faculty of Science, University of Tabuk, Tabuk, Saudi Arabia

[6]Biodiversity Genomics Unit, Faculty of Science, University of Tabuk, Tabuk, Saudi Arabia

[7]Department of Biomedical, Surgical and Dental Sciences, University of Milan, Milan, Italy

[8]National Interuniversity Consortium of Materials Science and Technology, Firenze, Italy

[†]*These authors contributed equally to this work.*

***Corresponding authors:**
Abdur Rauf
(abdurrauf@uoswabi.edu.pk)
Marcello Iriti
(marcello.iriti@unimi.it)

Citation: Rauf A, Ho S, Khan MU, *et al.* Anticancer potential of flavonoids isolated from *Pistacia chinensis* against glioblastoma (U87) cell line: Extensive *in vitro* and *in silico* research. *Eurasian J Med Oncol.* 2025;9(1):144-158. doi: 10.36922/ejmo.5768

Received: November 5, 2024

1st revised: December 19, 2024

2nd revised: January 1, 2025

Accepted: January 7, 2025

Published online: January 23, 2025

Copyright: © 2025 Author(s). This is an Open Access article distributed under the terms of the Creative Commons Attribution License, permitting distribution, and reproduction in any medium, provided the original work is properly cited.

Publisher's Note: AccScience Publishing remains neutral with regard to jurisdictional claims in published maps and institutional affiliations.

Abstract

Glioblastoma multiforme (GBM) poses significant challenges due to its aggressiveness and resistance to standard therapies, necessitating novel treatments. This study evaluates the anticancer potential of flavonoids isolated from *Pistacia chinensis* against the glioblastoma U87 cell line. Two flavonoids, 2-(3,4-dihydroxyphenyl)-5,7-dihydroxy-4H-chromen-4-one (Compound 1) and 2-(3,4-dihydroxyphenyl)-7,8-dihydroxy-3-methoxy-4H-chromen-4-one (Compound 2), were isolated using column chromatography and analyzed through *in silico* techniques, including molecular docking, density functional theory (DFT), and pharmacokinetic profiling. *In vitro* studies revealed dose- and time-dependent cytotoxicity, with Compound 1 demonstrating higher activity, reducing U87 cell viability by up to 70.11% after 48 h at 75 µg/mL. Molecular docking demonstrated its strong binding affinity to mTOR (−10.391 kcal/mol), while DFT confirmed its structural stability. Both compounds displayed favorable absorption, distribution, metabolism, excretion, and toxicity (ADMET) profiles, supporting their potential as therapeutic candidates. These findings underscore the significant anti-GBM activity of flavonoids, particularly Compound 1, warranting further *in vivo* studies to explore their clinical potential as effective GBM treatments.

Keywords: *Pistacia chinensis*; Flavonoids; Cancer; *In silico*; Molecular docking; Density functional theory; ADMET

1. Introduction

The early 19th century marked a pivotal era in the study of medicinal plants, revolutionizing pharmaceutical science and laying the groundwork for the discipline of modern pharmacology. This period witnessed significant advancements in identifying, validating, and extracting key alkaloids from various plants, which transitioned traditional herbal remedies into scientifically validated therapeutic agents. Milestones of this era included the extraction of morphine from poppy in 1806, strychnine and emetine from ipecacuanha in 1817, quinine from cinchona bark in 1820, and pelletierine from pomegranate in 1878.[1,2] These discoveries were instrumental in transforming how plants were used in medicine, advancing our understanding of their therapeutic properties. Glycosides were among the first compounds to be isolated, followed by other significant constituents such as tannins, saponosides, essential oils, vitamins, and hormones as chemical techniques evolved.[3]

Historically, humans have utilized medicinal plants for thousands of years, relying on natural remedies such as tinctures, teas, powders, and poultices made from raw plant materials.[4] Knowledge of these plants and their applications for treating ailments was traditionally passed down orally from generation to generation.[5,6] Over time, this wisdom was documented in herbal pharmacopeias, transforming the oral traditions into written records that provided detailed information on plants for conditions such as testicular cancer, lymphoma, lung cancer, and leukemia.[7] Modern allopathic medicine has its roots in these ancient practices, and it is expected that the fusion of traditional knowledge with contemporary scientific approaches will lead to the discovery of many new treatments.[8,9] Despite the progress in scientific validation, in many regions, the use of medicinal plants remains linked to superstitions and misconceptions, primarily due to the lack of empirical evidence to explain and predict their healing properties.[10]

Pistacia chinensis is a noteworthy species in the realm of medicinal plants belonging to the *Anacardiaceae* family. This small deciduous tree is native to China and North America, where it serves not only as a shade and ornamental garden tree but also holds significant therapeutic potential.[11] In traditional Chinese medicine, seed oil has long been used for medicinal purposes. In the United States of America, it has gained recognition for its potential in biodiesel production and remarkable insect resistance.[12] The chemical profile of *P. chinensis* predominantly includes flavonoids and phenolic compounds, which are known for their diverse biological activities, such as anti-inflammatory, hypoglycemic, anti-atherogenic, anti-oxidant, and insecticidal effects.[13-16] Several species within the *Pistacia* genus have demonstrated these biological activities, underscoring the therapeutic potential of this group of plants. Despite these promising characteristics, research into the specific chemical constituents and bioactive properties of *P. chinensis* has been relatively limited.

Existing studies have identified unique chemical constituents in *P. chinensis*, such as two 4-aryl coumarin moieties (neoflavone) dimers with estrogen-like activity isolated from its leaves, along with phenolic compounds such as quercetin, 6-O-galloylarbutin-quercetin, gallic acid, and m-gallic acid.[17,18] In addition, novel compounds such as pyrrolidone derivatives and anthotaxies have been extracted from its tender burgeons, suggesting that *P. chinensis* holds untapped potential for therapeutic applications.[13]

In the modern era of drug development, *in silico* techniques have become integral to therapeutic research, allowing for the simulation of chemical interactions, optimization of molecular structures, and prediction of biological activities. These computational approaches significantly enhance the drug discovery process by streamlining the evaluation of pharmacological and toxicological properties, which traditionally required extensive experimental validation.[19] Such methodologies have accelerated the pace of drug discovery and improved the precision of identifying promising candidates for further development.

It is reported in the literature that gall extract is common practice in folk medicine, revealing the presence of alkaloids, terpenoids, flavonoids, and tannins. Alkaloids are known for their diverse biological roles, including analgesic, anti-inflammatory, antispasmodic, and bactericidal activities. In addition to alkaloids, the analgesic and anti-inflammatory properties of the gall extract might also be attributed to the presence of triterpenes, tannins, and flavonoids.[4]

Given the untapped potential of *P. chinensis*, this study aims to comprehensively explore its chemical composition and biological activity using a combination of *in vitro* and *in silico* methodologies. Our focus centers on evaluating its anti-cancer efficacy against the aggressive glioblastoma (U87) cell line, followed by detailed analyses of the binding affinities of its compounds to glioblastoma-specific targets. In addition, we aim to assess the pharmacological and molecular properties of these compounds, seeking to uncover novel therapeutic agents from this ancient yet scientifically promising species. This research aspires to bridge the gap between traditional medicinal knowledge and modern therapeutic innovation, ultimately contributing to the development of effective treatments for challenging malignancies like glioblastoma.

2. Methods

2.1. Plant collection

The bark of *P. chinensis* was collected from the area surrounding Hostel 02 at the University of Peshawar, Khyber Pakhtunkhwa, Pakistan. To ensure the authenticity of the plant material, Dr. Muhammad Ilays, the esteemed Director of the Botany Department at the University of Swabi, kindly verified its botanical identity. His expertise provided a crucial validation step, ensuring the credibility of the sample used in our study. The specimen, meticulously labeled as UOS/Bot-55, has been preserved in the department's herbarium, serving as a reference for future research and verification.

2.2. Extraction and isolation

The bark of *P. chinensis* underwent a meticulous preparation process to ensure the integrity of the plant material for further study. Initially, the bark was thoroughly washed with clean water to remove any surface impurities and was then air-dried in a shaded area to prevent any degradation from sunlight. A total of 7.34 kg of shade-dried bark were finely ground into a powder using a grinder, yielding 7.20 kg of powdered material. This finely processed bark was then immersed in methanol for 16 days to facilitate an exhaustive extraction of its bioactive compounds.

After the 16-day soaking period, the methanolic extract was carefully filtered to remove any solid residues and then concentrated using a rotary evaporator under controlled low temperatures and reduced pressure. This technique was employed to preserve the chemical integrity of the extract, resulting in a crude extract weighing 81.29 g.

The crude extract was subjected to a fractionation process using a separating funnel for further purification. This approach effectively separated the extract into distinct fractions: hexane (5.01 g), chloroform (17.12 g), ethyl acetate (6.43 g), and methanolic (32.98 g) fractions. The methanolic fraction, known for its enriched content of bioactive compounds, was then analyzed using thin-layer chromatography (TLC) to assess its chemical profile.

The methanolic fraction was processed through silica gel column chromatography to isolate the specific compounds. The column was eluted with a mixture of methanol and chloroform in a 4:96 ratio, a strategic choice facilitating the separation of the targeted compounds. This method led to the successful isolation of two distinct compounds, Compound 1 and Compound 2. The final purification of Compound 1 and Compound 2 having various functional groups (Figure 1), including hydroxyl, ketone, and ether, was achieved through recrystallization using a methanol and chloroform solution in a 1:1 ratio. This process yielded

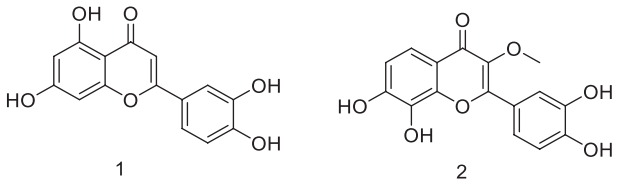

Figure 1. Chemical structure of Compounds 1 and 2, isolated from *Pistacia chinensis*

pure crystals of the compounds, ensuring their suitability for subsequent chemical and biological analyses.[20] This careful and methodical approach highlights the precision and thoroughness of our efforts to extract and purify the bioactive components of *P. chinensis*, paving the way for their potential application in therapeutic research.

2.3. Anti-cancer activity

To evaluate the inhibitory effects of the compounds on cell growth, the U87 cell line was initially chosen as a model, providing a reliable framework for assessing cytotoxicity. This step allowed us to systematically investigate the impact of specific bioactive compounds, identified as Compound 1 and Compound 2, on the suppression of cell proliferation. To quantify their cytotoxic potential, we employed the MTT assay, a well-regarded and extensively validated method for determining cell viability and measuring cytotoxic effects. This assay enabled a precise evaluation of the degree of growth inhibition imposed by these compounds on U87 cells, facilitating a comprehensive comparison of their relative efficacy in inhibiting tumor cell proliferation.[21]

2.4. *In silico* analysis

2.4.1. Retrieval of phytochemicals

The anti-cancer phytochemicals, identified as Compounds 1 and 2, underwent an extensive *in silico* analysis to explore their potential biological activities. Initially, their 2D and 3D structures were constructed using advanced molecular modeling tools. Specifically, ChemDraw Professional 16.0 software (version 16.0.1.4.77) was employed to create the 2D and 3D conformations using ChemDraw and Chem3D applications. These conformations were subsequently stored in both structure data file (SDF) and molecular (MOL) formats to facilitate further analyses, including docking simulations and density functional theory (DFT) evaluations.

2.4.2. Retrieval of target proteins

To identify the protein targets implicated in the anti-cancer activity of these compounds, we accessed the Protein Data Bank (PDB) (RCSB PDB: Homepage) database. Ten crucial protein targets known to play significant roles

in cancer progression were selected for analysis. These proteins included UPAR (PDB ID: 2FD6), P38 (PDB ID: 3ZYA), NRF (PDB ID: 4XMB), ERK (PDB ID: 5NHJ), mTOR (PDB ID: 5OQ4), STAT (PDB ID: 6NUQ), BCL-XL (PDB ID: 6RNU), MMP-9 (PDB ID: 4WZV), NRAS (PDB ID: 6ZIR), and AKT1 (PDB ID: 3O96). These targets were chosen based on specific criteria: they originate from *Homo sapiens*, possess a resolution of less than 3 Å, and are devoid of mutations, except for NRAS (PDB ID: 6ZIR). The proteins were downloaded in PDB format, while the co-crystal ligands (CCLs) of each protein were saved in SDF format for subsequent docking analyses.

2.4.3. Preparation of ligands

The ligands, including Compounds 1 and 2, along with the CCLs, were subjected to optimization using the Ligprep tool within Maestro, Schrodinger 2020-3 (version 12.5.139). The aim was to achieve energy-minimized 3D structures with accurate chiralities at a pH level of 7.0 ± 2 while maintaining default settings for consistency. To enhance the accuracy of the molecular modeling, the OPLS3e (Optimized Potentials for Liquid Simulations) force field was employed during the ligand minimization process, which significantly improved the conformational stability of the compounds.[22]

2.4.4. Preparation of proteins

Protein preparation was conducted using the Protein Preparation Wizard tool available in the Maestro interface of Schrodinger 2020-3 (version 12.5.139). Initially, each protein was individually imported into the workspace and underwent preprocessing, which involved filling in missing loops and chains using the Prime job module. Subsequent steps included the deletion of extra side chains and the assignment of zero-order bonds to metal atoms. Optimization was carried out at a specific pH of 7.0 ± 2, following the PROPKA predictions, to ensure optimal ionization states. In addition, water molecules located beyond 3 Å from the binding site were removed to refine the protein's active site environment. The final step involved energy minimization using the OPLS3e force field to ensure the protein's stability for docking procedures.[23]

2.4.5. Receptor grid generation

Receptor grid generation was a critical step in the docking process, executed using Maestro's Receptor Grid Generation tool. The active binding site of each protein-ligand complex was pinpointed, and the grid was centered on the centroid of the CCL for each target protein. To refine this grid, a scaling factor of 1.0 was applied to the van der Waals radii alongside a partial charge cutoff of 0.25. The default parameters were maintained for site constraints, rotatable groups, and excluded volumes, ensuring an optimized environment for ligand docking.[24]

2.4.6. Molecular docking

Molecular docking was conducted to explore the interaction dynamics between the ligands and their respective protein targets. This was accomplished using the Glide module within the Maestro interface of Schrodinger 2020-3. Both Compounds 1 and 2, along with the CCLs, were subjected to flexible docking simulations using the energy-minimized conformations derived from the earlier steps. The docking mode was set to extra precision (XP), which is designed to yield highly reliable binding affinity predictions. In addition, the root mean square deviation (RMSD) was calculated for the input ligand geometries to validate the accuracy of the docking procedure.[23] Finally, the top-scoring ligands were visualized in the BIOVA Discovery Studio Visualizer (version 21.1.0.20298), enabling a detailed examination of the molecular interactions within the active site of each target protein and providing valuable insights into their binding mechanisms.

2.4.7. Prediction of absorption, distribution, metabolism, and excretion properties

Understanding the absorption, distribution, metabolism, and excretion (ADME) characteristics of phytochemicals is a crucial step in the drug discovery process. These pharmacokinetic properties play a vital role in determining the effectiveness of a potential therapeutic agent's effectiveness, as many drug candidates fail due to unfavorable ADME profiles, leading to issues in drug development and clinical outcomes.[25] To mitigate these risks and ensure the viability of the compounds, we conducted a comprehensive ADME analysis following the molecular docking studies.

For this purpose, we utilized SwissADME, an advanced tool specifically designed to assess the pharmacokinetic attributes of chemical compounds. The 2D molecular structures of the phytochemicals were transformed into Simplified Molecular Input Line Entry System (SMILES) strings, providing a simplified yet highly precise representation of their chemical makeup. This conversion enabled a more rigorous and detailed analysis of the compounds' potential drug-like properties. During this evaluation, each phytochemical was systematically screened against Lipinski's Rule of Five (LRF), a widely recognized standard that predicts the oral bioavailability of chemical entities based on key molecular parameters, such as molecular weight, lipophilicity, hydrogen bond donors, and acceptors.[26]

Multiple models, including iLOGP, XLOGP3, WLOGP, MLOGP, and SILICOS-IT, assessed lipophilicity. The consensus log $P_{o/w}$ was determined to predict membrane permeability and interaction potential. Water solubility was calculated using ESOL, Ali, and SILICOS-IT models, with log S values guiding the prediction of oral bioavailability.

Medicinal chemistry filters, such as PAINS and Brenk, were applied to identify structural alerts, while synthetic accessibility scores predicted the ease of compound synthesis. Drug likeness was further evaluated using LRF, Ghose, Veber, and Egan criteria, alongside bioavailability scores. Skin permeability coefficients (log k_p) were also calculated to assess absorption potential.

This approach not only enhanced our understanding of the drug-like behavior of the phytochemicals but also identified any possible limitations that could hinder their development as therapeutic agents. By ensuring that the compounds met these stringent criteria, we paved the way for their potential progression to the next phases of drug development, reducing the likelihood of costly failures at later stages.

2.4.8. Toxicity assessment

Toxicity assessment is an essential stage in effective drug development, as it evaluates the potential harmful effects of compounds on living organisms.[27] In our current research, we undertook a comprehensive toxicity evaluation using two advanced tools: the Pharmacokinetics and Toxicity Prediction (PkCSM; uq.edu.au) online server and StopTox (unc.edu).

The PkCSM online server provides a robust platform for assessing toxicity through various parameters presented in both binary yes/no formats and specified units.[28] This dual approach enables a nuanced understanding of the toxicological profile of the compounds, allowing researchers to identify any concerning attributes early in the development process.

In addition, we employed StopTox, which incorporates a comprehensive "6-pack" assessment. This tool evaluates several critical toxicity endpoints, including acute oral toxicity, acute dermal toxicity, acute inhalation toxicity, irritation (skin and eye), skin corrosion, and skin sensitization.[29] By utilizing these sophisticated tools, we aimed to ensure that any potential drug candidates exhibit acceptable safety profiles, thereby mitigating risks associated with their development and potential clinical application.

2.4.9. Bioactivity evaluation

The bioactivity of the isolated phytochemicals was thoroughly evaluated using the Molinspiration Cheminformatics tool "Calculation of molecular properties and bioactivity score" (molinspiration.com), which is renowned for its ability to calculate molecular properties and bioactivity scores.[30] This comprehensive analysis focused on various key biological targets, including G protein-coupled receptors (GPCRs), ligand modulators for ion channels, nuclear receptor ligands, kinase inhibitors, protease inhibitors, and enzyme inhibitors.

To perform this assessment, the phytochemicals, saved in MOL format, were submitted as input files into the Molinspiration platform. This facilitated the computation of bioactivity scores, allowing us to gain insights into the potential efficacy and interaction of these compounds with the targeted biological pathways. The results from this evaluation are critical for understanding the therapeutic potential of the phytochemicals and guiding further research into their pharmacological applications.

2.4.10. DFT calculations

To explore the molecular characteristics of the isolated phytochemicals, we employed DFT using the B3LYP method in conjunction with a 3-**2**1G basis set. This computational approach allowed us to determine the optimized molecular conformations of both compounds in their energy-minimized ground states. The visualizations of these optimized structures were carried out using GaussView 5.0.8 software and the Gaussian 09W program.[30]

In addition to structural optimization, we investigated the frontier molecular orbitals (FMO), molecular electrostatic potential (MEP), and various chemical reactivity descriptors, as established by Koopman's theorem.[31] The FMO cubes were further visualized using VESTA (version 3), enhancing the computational clarity of our findings. This multifaceted approach provides valuable insights into the electronic properties of the phytochemicals, contributing to a deeper understanding of their potential biological activities and interactions.

3. Results

3.1. *In vitro* results

The anticancer activity of compounds isolated from *P. chinensis* was systematically evaluated using the glioblastoma (U87) cell line, focusing on varying concentrations (25, 50, and 75 μg/mL) and time points (24 and 48 h). The results, summarized in Table 1, reveal a compelling dose- and time-dependent inhibition of cell viability by both compounds.

At a concentration of 25 μg/mL, Compound 1 exhibited a modest reduction in cell viability after 24 h of treatment, with an inhibition rate of 10.11%. Notably, this inhibitory

effect significantly escalated after 48 h, reaching 60.34% ($P < 0.05$). Increasing the concentration to 50 µg/mL led to an improvement in the 24-h inhibitory activity, recorded at 14.35%, which further amplified to 65.23% at the 48-h mark ($P < 0.01$). At the highest concentration tested (75 µg/mL), Compound 1 demonstrated enhanced anti-cancer efficacy, resulting in a 14.98% reduction in viability after 24 h and increasing to 70.11% after 48 h ($P < 0.001$).

Compound 2 exhibited a similar pattern of dose-dependent inhibition. At 25 µg/mL, the compound displayed an inhibition of 9.54% at 24 h, which significantly increased to 55.09% after 48 h ($P < 0.05$). The intermediate concentration of 50 µg/mL induced a more pronounced effect, reducing cell viability by 16.09% after 24 h and achieving 61.54% inhibition after 48 h ($P < 0.01$). At the highest concentration (75 µg/mL), Compound 2 exhibited the strongest inhibitory effect, with a marked reduction in cell viability to 30.06% at 24 h, further reaching 68.98% after 48 h ($P < 0.001$).

Table 1. Anti-cancer activity of compounds isolated from *Pistacia chinensis* in the glioblastoma (U87) cell line

Sample	Dose (µg/mL)	Time (h)	
		24	48
Compound 1	25	10.11	60.34
	50	14.35	65.23
	75	14.98	70.11
Compound 2	25	9.54	55.09
	50	16.09	61.54
	75	30.06	68.98

In general, both compounds demonstrated potent anti-cancer activity against the U87 glioblastoma cell line, demonstrating increased efficacy with higher concentrations and prolonged exposure times. These findings highlight the promising potential of these isolated compounds as therapeutic agents in the treatment of glioblastoma.

3.2. *In silico* results

The 2D and 3D structures, as well as the SMILES notations of the phytochemicals extracted from *P. chinensis*, are summarized in Table 2. These two bioactive compounds, designated as Compound 1 and Compound 2, underwent comprehensive *in silico* studies to elucidate their molecular characteristics and potential bioactivity.

These conformations and their respective SMILES representations provide valuable insights into the molecular properties and facilitate further computational analyses, including docking studies and ADME evaluations. The detailed structural information plays a critical role in understanding the pharmacological potential of these phytochemicals.

Table 2. 2D and 3D conformations of bioactive flavonoids (Compounds 1 and 2), with the corresponding Simplified Molecular Input Line Entry System (SMILES) string

Compound	Compound	2D structure	3D structure	SMILES
1	2-(3,4-dihydroxyphenyl)-5,7 -dihydroxy-4H-chromen-4-one	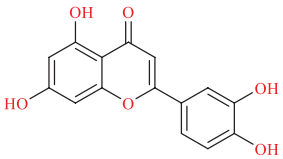	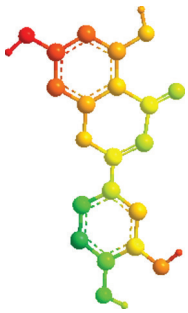	O=C1C2=C (O) C=C (O) C=C2OC (C3=CC (O)=C (O) C=C3)=C1
2	2-(3,4-dihydroxyphenyl)-7,8-dihydroxy -3-methoxy-4H-chromen-4-one	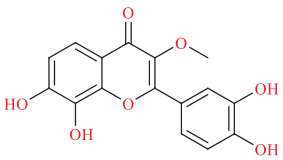	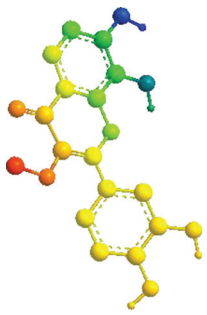	COC1=C (C2=CC=C (O) C (O)=C2) OC3=C (O) C (O)=CC=C3C1=O

3.3. Molecular docking

Molecular docking was conducted in XP mode for both phytochemicals (Compound 1 and Compound 2) against 10 target proteins, identified by their respective PDB IDs: 2FD6, 3ZYA, 4XMB, 5NHJ, 5OQ4, 6NUQ, 6RNU, 4WZV, 6ZIR, and 3O96. The initial step in the docking process involved verifying the docking protocol by calculating the all-atom RMSD of the original control ligand (CCL) and the redocked CCL for all target proteins. The resulting RMSD values were ≤ 2 Å for all proteins, confirming the validity of the docking protocol.

The docking results are presented in Table 3, which illustrates the docking scores of the bioactive flavonoids (Compounds 1 and 2) in comparison to their control ligands (CCLs). Notably, Compound 1 achieved the highest docking scores against most of the target proteins.

Remarkably, Compound 1 exhibited the highest docking score of −10.391 kcal/mol against mTOR (PDB ID: 5OQ4), while Compound 2 achieved a score of −10.28 kcal/mol against the same target. Conversely, Compound 2 emerged as a top scorer against AKT1 (PDB ID: 3O96) with a score of -10.458 kcal/mol. The docking scores suggested that Compounds 1 and 2 have strong binding interactions against mTOR and AKT1, respectively.

The strong binding affinities of both compounds were further visualized using Discovery Studio, as depicted in Figure 2.

Figure 2A illustrates the interactions of Compound 2 with AKT1 (PDB ID: 3O96), highlighting the formation of two conventional hydrogen bonds between amino acid residues Thr211 and Ser205 with the hydroxyl groups (-OH) positioned at the ortho position of the catechol benzene ring. In contrast, Figure 2C demonstrates that the CCL formed a single hydrogen bond with Tyr272 and cyclohexylamine, indicating greater stability for Compound 2 within the complex with 3O96. In addition, hydrophobic interactions were observed between Compound 2 and the CCL; specifically, the residue Trp80 formed hydrophobic π-π stacking interactions with hydroxy-dihydro-pyranone and the aromatic moiety of the ring. Moreover, hydrophobic π-alkyl interactions were identified with residues Val270 and Leu210. The following residues contributed to van der Waals interactions: Ala212, Leu213, Arg206, Tyr263, His207, Leu264, Lys268, Gln79, Asn54, Val271, Tyr273, and Asp292. These interactions collectively enhance the stability of the Compound 2 complex, suggesting that it may serve as a superior inhibitor compared to the CCL against the AKT1 protein. These findings collectively highlighted the potential of Compound 1 and Compound 2 as promising inhibitors of glioblastoma-related targets, specifically mTOR and AKT1, which are critical for glioblastoma progression.

Table 3. Docking scores of bioactive flavonoids (Compounds 1 and 2) against 10 putative glioblastoma target proteins, compared with their co-crystal ligands (CCLs)

Target proteins	Docking scores (kcal/mol)		
	CCL	1	2
2FD6	−3.914	−3.923	−2.885
3ZYA	−12.131	−9.034	−6.914
4WZV	−9.253	−9.096	−7.959
4XMB	−9.017	−6.894	−6.646
5NHJ	−11.889	−10.185	−8.502
5OQ4	−8.484	−10.391	−10.28
6NUQ	−7.86	−3.911	−4.787
6RNU	−5.404	−6.824	−7.152
6ZIR	−3.028	−2.717	−3.999
3O96	−10.086	−10.208	−10.458

Figure 2B displays the interaction of Compound 1 with mTOR (PDB ID: 5OQ4), showcasing the hydrogen bond formations between residue Glu880 and one of the -OH groups attached to the catechol, as well as between residue Val882 and both -OH groups of catechol. Furthermore, residues Asp836 and Lys833 formed hydrogen bonds with the -OH group of phenol and the oxygen of the ether attached to the aromatic ring, suggesting enhanced binding affinity and stability of the complex. Notably, Lys833 also participated in the formation of hydrophobic π-alkyl interactions with other amino acid residues. An electrostatic π-sulfur interaction was identified, formed by residue Met953 within the benzoid moiety of the ring, which plays a critical role in stabilizing the complex. In contrast, in the CCL (Figure 2D), only conventional hydrogen bonds and π-alkyl interactions were observed, with the van der Waals forces being more prominent in the Compound 1 complex than in the CCL. These findings indicate that Compound 1 holds promise as a potential inhibitor for the mTOR protein.

3.4. Prediction of absorption, distribution, metabolism, and excretion properties

The evaluation of the physicochemical properties of Compounds 1 and 2 (Table 4) indicates compliance with LRF. Specifically, the molecular weights of both compounds are ≤500 g/mol, the number of hydrogen bond donors is ≤5, and the number of hydrogen bond acceptors is ≤10. In addition, the total polar surface area (TPSA) is ≤140 Å² for both phytochemicals, suggesting their potential as drug-like candidates.

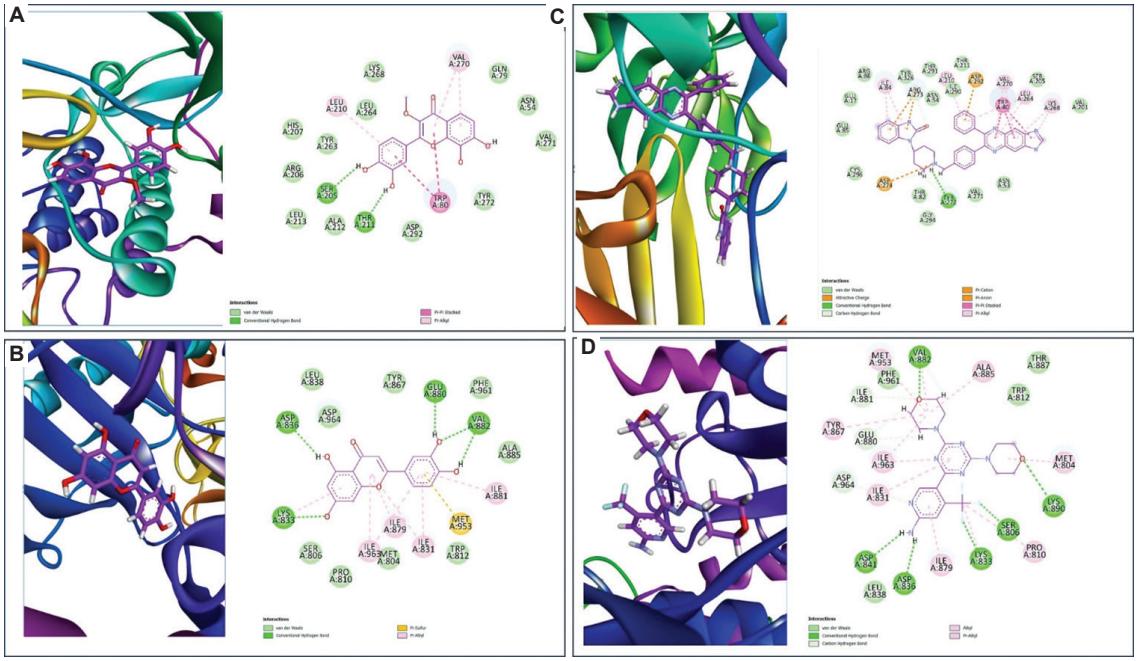

Figure 2. 2D interactions between ligand and amino acid residues along with 3D conformation of ligands within the binding cavity. (A) Visual representation of Compound 2 within the binding pocket of AKT1 (3O96). (B) Visual representation of Compound 1 within the binding pocket of mTOR (PDB ID: 5OQ4). (C) Visual representation of co-crystal ligand (CLL) within the binding pocket of AKT1 (PDB ID: 3O96). (D) Visual representation of CCL within the binding pocket of mTOR (PDB ID: 5OQ4).
Abbreviation: PDB: Protein Data Bank.

Table 4. Pharmacological evaluation of bioactive flavonoids (Compounds 1 and 2) based on various parameters, accessed through SwissADME

Physiochemical properties						
Compound	**Molecular weight (g/mol)**	**No. of heavy atoms**	**No. of rotatable bonds**	**H-bond acceptors**	**H-bond donors**	**TPSA (Å)**
1	286.24	21	1	6	4	111.13
2	316.26	23	2	7	4	120.36
Lipophilicity						
Compound	**Log $P_{o/w}$ (iLOGP)**	**Log $P_{o/w}$ (XLOGP3)**	**Log $P_{o/w}$ (WLOGP)**	**Log $P_{o/w}$ (MLOGP)**	**Log $P_{o/w}$ (SILICOS-IT)**	**Consensus log $P_{o/w}$**
1	1.86	2.53	2.28	−0.03	2.03	1.73
2	1.59	1.94	2.29	−0.31	2.06	1.52
Water solubility and medicinal chemistry						
Compound	**Log S (ESOL)**	**Log S (Ali)**	**Log S (SILICOS-IT)**	**PAINS**	**Brenk**	**Synthetic accessibility**
1	−3.71	−4.51	−3.82	1	1	3.02
2	−3.41	−4.09	−3.94	1	1	3.28
Drug-likeness						
Compound	**Lipinski**	**Ghose**	**Veber**	**Egan**	**Bioavailability score**	**Log K_p (cm/s)**
1	Yes	Yes	Yes	Yes	0.55	−6.25
2	Yes	Yes	Yes	Yes	0.55	−6.85

Abbreviations: H-bond: Hydrogen Bond; Log: Logarithm; Log Kp: Skin permeability coefficient; Log S: Logarithm of solubility; o/w: Octanal-water partition; PAIN: Pan-Assay Interference Compound; TPSA: Total polar surface area.

3.5. Lipophilicity and water solubility

The lipophilicity and water solubility of the phytochemicals are represented by their log $P_{o/w}$ values. Compound 1 exhibited superior lipophilicity with a consensus log $P_{o/w}$ of 1.73 compared to Compound 2's value of 1.52. In contrast, Compound 2 demonstrated enhanced water solubility, as indicated by its log S value of 3.94, in comparison to Compound 1's log S of 3.82 (Table 4).

3.6. Drug-likeness assessment

The drug-likeness of both phytochemicals (Compounds 1 and 2) was evaluated according to Lipinski, Ghose, Veber, and Egan rules. As outlined in Table 4, neither phytochemical violated any of the specified rules. The medicinal chemistry evaluation revealed one PAINS (Pan-Assay Interference Compound) and one Brenk alert for both phytochemicals. Furthermore, the synthetic accessibility analysis indicated that Compound 1, with a score of 3.02, is easier to synthesize than Compound 2, which has a score of 3.28.

3.7. Pharmacokinetic evaluation

The pharmacokinetic properties of both phytochemicals were further assessed using the BOILED-EGG model, depicted in Figure 3. Both compounds demonstrated high gastrointestinal (GI) absorption potential. Notably, neither compound was identified as a substrate for P-glycoprotein (PGP-negative), suggesting that the pharmacological activity of both phytochemicals will remain unaffected by PGP. Despite both phytochemicals having a bioavailability score of 0.55, this indicates a moderate level of oral bioavailability within the physicochemical space.

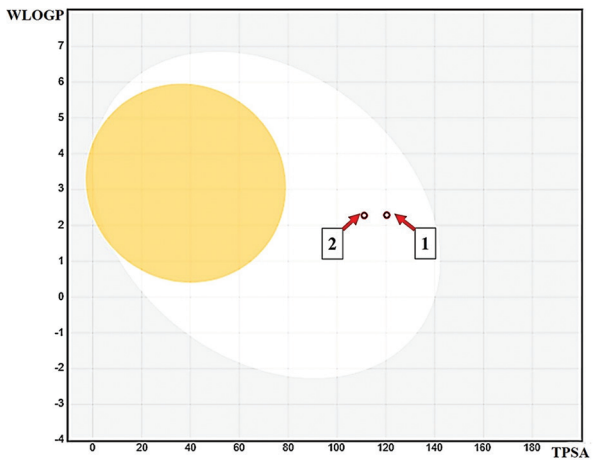

Figure 3. Brain Or IntestinaL EstimateD permeation (BOILED-Egg) representation of bioactive flavonoids (Compounds 1 and 2) of *Pistacia chinensis*

3.8. Toxicity assessment

The toxicity assessment for the phytochemicals was conducted using the PkCSM server, as summarized in Table 5. The results indicated that Compound 1 demonstrated non-toxic characteristics across several toxicity models, including Ames toxicity, hepatotoxicity, hERG I and II inhibitors, and skin sensitization, where it remained inactive. In contrast, Compound 2 displayed potential Ames toxicity, suggesting possible carcinogenic effects.

3.8.1. Maximum tolerated dose and toxicity levels

The maximum tolerated doses were calculated to be 0.839 log mg/kg/day for Compound 1 and 1.023 log mg/kg/day for Compound 2. This suggests that Compound 2 is more tolerant at higher doses. In addition, Compound 2 exhibited lower toxicity to both *Minnow* and *Tetrahymena pyriformis*, indicating a more favorable toxicity profile in aquatic environments. However, the oral rat acute and chronic toxicity assessments revealed that both phytochemicals exhibited similar levels of chronic toxicity, with Compound 1 having a slightly lower acute toxicity (2.235 mol/kg) compared to Compound 2 (2.347 mol/kg).

3.8.2. Further toxicity evaluation using StopTox

The toxicity of both phytochemicals was also evaluated through the StopTox platform, as illustrated in Table 6. The results indicated that both compounds exhibited a non-toxic

Table 5. Toxicity prediction of bioactive flavonoids (Compounds 1 and 2) across various parameters, accessed through PkCSM

Toxicity assessment	Phytochemicals	
	Compound 1	Compound 2
Ames toxicity	No	Yes
Maximum tolerated dose, human (log mg/kg/day)	0.839	1.023
hERG I inhibitor	No	No
hERG II inhibitor	No	No
Oral rat acute toxicity, LD50 (mol/kg)	2.235	2.347
Oral rat chronic toxicity, LOAEL (log mg/kg bw/day)	2.052	2.035
Hepatotoxicity	No	No
Skin sensitization	No	No
T.Pyriformis toxicity (log µg/L)	0.361	0.302
Minnow toxicity (log mM)	0.87	1.214

Abbreviations: hERG I: *Human Ether-à-go-go-Related Gene, type I;* hERG II: Human Ether-à-go-go-Related Gene, type II; LD: Lethal dose; LOAEL: Lowest observed adverse effect level; *T. pyriformis: Tetrahymena pyriformis.*

Table 6. Toxicity evaluation of bioactive flavonoids (Compounds 1 and 2) across various parameters, accessed through StopTox

Compound	Acute inhalation toxicity	Acute oral toxicity	Acute dermal toxicity	Eye irritation and corrosion	Skin sensitization	Skin irritation and corrosion
1	Non-toxic	Non-toxic	Toxic	Non-toxic	Sensitizer	Negative
2	Non-toxic	Non-toxic	Toxic	Toxic	Sensitizer	Negative

profile concerning acute inhalation and oral toxicity. Notably, neither compound elicited skin irritation or corrosion. However, Compound 2 displayed the potential for eye irritation and corrosion. Both compounds were identified as possessing dermal toxicity and skin sensitization.

3.9. Bioactivity evaluation

The computed bioactivity scores for Compounds 1 and 2 are summarized in Table 7. These scores are interpreted according to established guidelines: active scores are defined as >0, moderately active scores range from -5.0 to 0.0, and inactive bioactivity scores are < -5.0. The findings revealed that Compound 1 exhibited greater activity as a nuclear receptor ligand (0.39), kinase inhibitor (0.26), and enzyme inhibitor (0.28) compared to Compound 2. In addition, both phytochemicals demonstrated moderate activity as GPCR ligands, ion-channel modulators, and protease inhibitors. Overall, Compound 1 appears to be a more promising candidate regarding bioactivity.

3.10. DFT analysis

The DFT analysis of Compounds 1 and 2 was performed to understand their electronic properties and reactivity using Koopman's theorem. The computed electronic energies and reactivity parameters are summarized in Table 8. Both compounds exhibited similar energy gaps (0.91 eV for Compound 1 and 0.90 eV for Compound 2) and hardness values (-0.45 eV), suggesting their comparable stability in a molecular context. The key findings are as follows:

(i) Stability and reactivity: Compound 1 demonstrated a lower ionization potential (6.16 eV) and a higher electron affinity (5.25 eV) compared to Compound 2, indicating that Compound 1 has a lesser tendency to lose electrons and a stronger capability to accept electrons, contributing to its overall stability and higher reactivity.

(ii) Electronegativity and electrophilicity: Compound 1 displayed greater electrophilicity (-35.85 eV) and electronegativity (5.70 eV), highlighting its propensity for electron acceptance, thus making it more reactive compared to Compound 2.

(iii) Dipole moment: The lower dipole moment observed in Compound 2 (1.99 Debye) compared to Compound 1 (2.95 Debye) indicates that Compound 1 has a more polar nature, which could potentially influence its interactions with biological targets.

Table 7. Bioactivity scoring of bioactive flavonoids (Compounds 1 and 2) across various bioactivity parameters, access through Molinspiration

Bioactivity parameters	Bioactivity scores	
	Compound 1	Compound 2
GPCR ligand	−0.02	−0.16
Ion channel modulator	−0.07	−0.25
Kinase inhibitor	0.26	0.14
Nuclear receptor ligand	0.39	0.04
Protease inhibitor	−0.22	−0.35
Enzyme inhibitor	0.28	0.16

Abbreviation: GPCR: G-protein coupled receptor

Table 8. Chemical reactivity parameter of bioactive flavonoids (Compounds 1 and 2) computed through Koopman's theorem

Parameters for DFT analysis	Compound 1	Compound 2
Dipole moment (Debye)	2.9540	1.9900
HOMO (eV)	−6.1534	−5.2983
LUMO (eV)	−5.2491	−4.3998
Energy gap (ΔE_{Gap})	−0.91	−0.90
Ionization potential, *I* (eV)	6.16	5.30
Electron affinity (eV)	5.25	4.40
Electronegativity, χ (eV)	5.70	4.85
Electrochemical potential, μ (eV)	−5.70	−4.85
Hardness, η (eV)	−0.45	−0.45
Softness, S (eV)	−2.20	−2.23
Electrophilicity, ω (eV)	−35.85	−26.17

Abbreviations: DFT: Density functional theory; HOMO: Highest occupied molecular orbital; LUMO: Lowest unoccupied molecular orbital.

These findings imply that Compound 1 has a more favorable electronic structure and reactivity profile, positioning it as a potentially more suitable drug candidate when evaluated based on its chemical reactivity parameters.

3.11. MEP mapping

The MEP mapping of the optimized structures for both compounds (Figure 4) provides insight into their

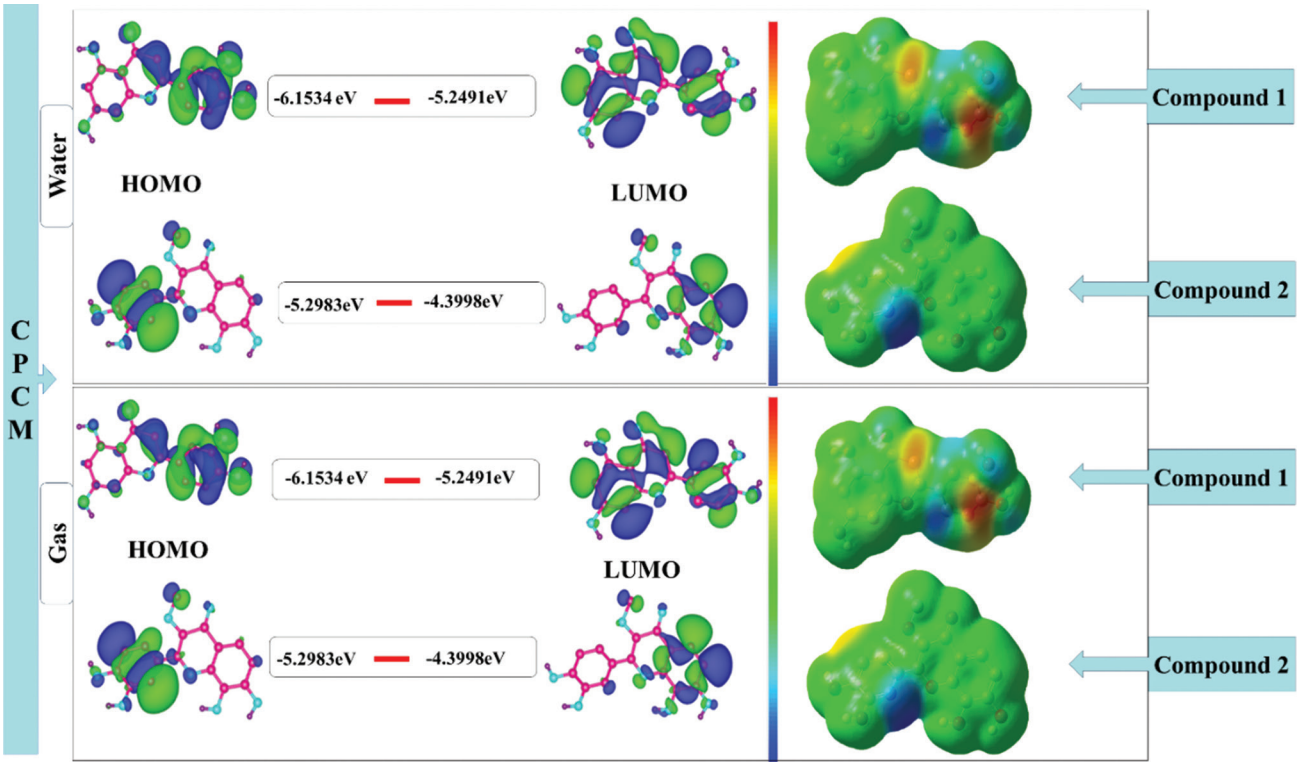

Figure 4. Molecular electrostatic potential (MEP) mapping of optimized structural geometries. The optimized structural geometries of Compounds 1 and 2 were analyzed using the conductor-like polarizable continuum model (CPCM) and visualized with Vesta software. The color-coded MEP mapping reinforces the potential for both compounds to engage in specific interactions with various molecular targets.
Abbreviations: HOMO: Highest occupied molecular orbital; LUMO: Least unoccupied molecular orbital.

electrophilic and nucleophilic regions. The MEP map color-coded representation indicates:

(i) Red regions depict areas with high negative potential, favoring electrophilic attacks.
(ii) Blue regions denote regions of high positive potential, favoring nucleophilic attacks.
(iii) Green regions represent neutral zones, where neither electrophilic nor nucleophilic reactions are particularly favored.

These mappings suggest that both compounds exhibit well-defined electrophilic and nucleophilic regions, highlighting their potential for efficient orbital interactions with biological macromolecules, which can enhance their pharmacodynamic properties.

4. Discussion

This study emphasizes the therapeutic potential of *P. chinensis*, specifically its anti-cancer efficacy against glioblastoma (U87) cells. Various species within the *Pistacia* genus have been explored for their pharmacological effects, including anti-inflammatory, hypoglycemic, and hepatoprotective activities, and they possess anti-phosphodiesterase-1, antiglycation, antioxidant, and lipoxygenase inhibitory properties as well.[14-16,32-34] The bioactive compounds derived from *P. chinensis* remain largely unexamined in cancer research. Our investigation seeks to bridge this gap by evaluating the cytotoxic effects of two flavonoids isolated from the methanolic extract of *P. chinensis* and analyzing their drug-like properties through *in silico* assessments.

The study's findings revealed notable cytotoxicity from two flavonoids, 2-(3,4-dihydroxyphenyl)-5,7-dihydroxy-4H-chromen-4-one (Compound 1) and 2-(3,4-dihydroxyphenyl)-7,8-dihydroxy-3-methoxy-4H-chromen-4-one (Compound 2) against glioblastoma cells, with a dose- and time-dependent reduction in cell viability. Notably, at a concentration of 75 µg/mL, Compound 1 exhibited up to 70.11% inhibition in cell viability at 48 h, surpassing the 68.98% inhibition exhibited by Compound 2. These results highlight the promising potential of *P. chinensis* as a source of plant-based chemotherapeutic agents, suggesting these flavonoids are viable candidates for further development in cancer therapy.

The bioactivity of these flavonoids is closely associated with the chemical properties of *P. chinensis*. Flavonoids have been widely reported for their anti-oxidant, anti-

inflammatory, and anti-cancer activities, and these isolated compounds share structural similarities with neoflavones, which have estrogen-like activity and potential cancer cell proliferation inhibition.[35] The cytotoxic activity observed aligns with the established molecular mechanisms of flavonoids in inducing apoptosis and disrupting critical signaling pathways in cancer cells.

Furthermore, several phenolic constituents from *P. chinensis*, such as quercetin, gallic acid, and arbutin derivatives,[36] have demonstrated robust anti-cancer properties, supporting the hypothesis that this plant's diverse chemical profile may contribute synergistically to its biological activities. These observations are consistent with earlier studies on other *Pistacia* species, such as *Pistacia lentiscus* and *Pistacia atlantica*, which have demonstrated anti-cancer effects against various cell lines, thereby expanding the scientific understanding of this genus's therapeutic scope.[37-40]

Comparative analysis with other plant-derived flavonoids and phenolic compounds suggests that the flavonoids from *P. chinensis* exhibit either comparable or superior cytotoxicity against glioblastoma cells. This implies that these compounds might exert their anti-cancer effects through mechanisms involving the induction of apoptosis, cell cycle arrest, and interference with tumor-promoting signaling pathways.[41,42]

The study also incorporated *in silico* analysis, revealing significant binding affinities of Compound 1 (-10.319 kcal/mol) and Compound 2 (-10.458 kcal/mol) toward the mTOR (PDB ID: 5OQ4) and AKT1 (PDB ID: 3O96) proteins, respectively. These interactions underscore their potential as mTOR/AKT pathway inhibitors, aligning with the observed effects of other natural compounds, like luteolin, in glioblastoma inhibition.[43,44] In addition, absorption, distribution, metabolism, excretion, and toxicity (ADMET) profiling indicated favorable drug-like characteristics for both compounds, with high gastrointestinal absorption and moderate bioavailability despite limited blood–brain barrier (BBB) permeability. This limitation might be mitigated through conjugation with BBB-crossing inhibitors, enhancing their clinical applicability.

Quantum chemical analysis through DFT further supported the molecular stability and reactivity of these flavonoids, particularly Compound 1, which exhibited superior electronic properties conducive to strong protein-ligand interactions. These results resonate with existing studies employing DFT calculations to elucidate the molecular characteristics of natural compounds, suggesting promising lead candidates for anti-cancer therapy.[45-48]

Future directions for this research should include detailed mechanistic studies to fully understand the pathways through which these flavonoids exert their effects on glioblastoma cells. *In vivo* studies and combinational therapies using these compounds with conventional chemotherapeutic agents may reveal synergistic effects and address potential challenges like drug resistance.

5. Conclusion

This comprehensive investigation into the anti-cancer potential of *P. chinensis* highlights its significant therapeutic efficacy against glioblastoma cells. The flavonoids isolated from its methanolic extract demonstrated potent, dose-dependent cytotoxicity, and *in silico* analyses confirmed their drug-like properties, with Compound 1 emerging as particularly promising. These findings establish a strong basis for developing novel plant-based chemotherapeutic agents. Despite this promise, several challenges must be addressed to advance these compounds toward clinical application. Limited BBB permeability may restrict their therapeutic reach to glioblastoma tissues, while potential off-target effects necessitate careful toxicity profiling to ensure safety. In addition, chemical modifications may be required to enhance their bioavailability and clinical efficacy. Future research should focus on overcoming these limitations through advanced delivery systems, *in vivo* studies, and exploring these flavonoids in combination therapies. This work underscores the potential of *P. chinensis* as a valuable source of innovative cancer treatments and offers a roadmap for their development into clinically viable therapeutics.

Acknowledgments

None.

Funding

None.

Conflict of interest

Marcello Iriti is an Editorial Board Member of this journal but was not in any way involved in the editorial and peer-review process conducted for this paper, directly or indirectly. Separately, other authors declared that they have no known competing financial interests or personal relationships that could have influenced the work reported in this paper.

Author contributions

Conceptualization: Abdur Rauf, Soonmin Ho, Muhammad Umer Khan

Data curation: Zuneera Akram, Omar S. Bahattab

Formal analysis: Abdur Rauf, Zuneera Akram, Muhammad Umer Khan, Marcello Iriti
Investigation: Abdur Rauf, Iqra Khurram
Methodology: Iqra Khurram, Zuneera Akram
Supervision: Abdur Rauf, Soonmin Ho
Writing – original draft: Zuneera Akram, Omar S. Bahattab, Yahya S. Al-Awthan
Writing – review & editing: Abdur Rauf., Soonmin Ho, Marcello Iriti

Ethics approval and consent to participate

Not applicable.

Consent for publication

Not applicable.

Availability of data

All the data are available in the manuscript as well as with the corresponding author.

References

1. Fitzgerald M, Heinrich M, Booker A. Medicinal plant analysis: A historical and regional discussion of emergent complex techniques. *Front Pharmacol*. 2020;10:1480.

   doi: 10.3389/fphar.2019.01480

2. Srivastava AK. *Significance of medicinal plants in human life. In: Synthesis of Medicinal Agents from Plants*. Netherlands: Elsevier; 2018. p. 1-24.

3. Alamgir AN. *Therapeutic Use of Medicinal Plants and Their Extracts*. Vol. 1. Switzerland: Springer International Publishing AG; 2017.

   doi: 10.1007/978-3-319-63862-1

4. Chabattula SC, Gupta PK, Govarthanan K, *et al*. Anti-cancer activity of biogenic nat-zno nanoparticles synthesized using Nyctanthes arbor-tristis (Nat) flower extract. *Appl Biochem Biotechnol*. 2024;196(1):382-399.

   doi: 10.1007/s12010-023-04555-1

5. Panda H. *Handbook on Medicinal herbs With Uses: Medicinal Plant Farming, most Profitable Medicinal Plants in India, Medicinal Plants Farming in India, Plants Used in Herbalism, Medicinal Herbs You Can Grow, Medicinal Herbs and Their Uses, Medicinal Herbs, Herbal and Medicinal plants, Growing Medicinal Herb, Most Profitable Medicinal Herbs Growing with Small Investment, Herbal Medicine Herbs*. New Delhi: Asia Pacific Business Press Inc.; 2004. p. 1-550.

6. Leonti M. The future is written: Impact of scripts on the cognition, selection, knowledge and transmission of medicinal plant use and its implications for ethnobotany and ethnopharmacology. *J Ethnopharmacol*. 2011;134(3):542-555.

   doi: 10.1016/j.jep.2011.01.017

7. Ogidi OI. Recent advances in anticancer activity and bioinformatics approach from potential plants. In: *Computational Approaches in Biotechnology and Bioinformatics*. United States: CRC Press. p. 61-87.

8. More B. Overview of medicine-its importance and impact. *DJ Int J Med Res*. 2016;1(1):1-8.

   doi: 10.18831/djmed.org/2016011001

9. Sen S, Chakraborty R. Revival, modernization and integration of Indian traditional herbal medicine in clinical practice: Importance, challenges, and future. *J Tradit Complement Med*. 2017;7(2):234-244.

10. Tanaka MM, Kendal JR, Laland KN. From traditional medicine to witchcraft: Why medical treatments are not always efficacious. *PLoS One*. 2009;4(4):e5192.

    doi: 10.1371/journal.pone.0005192

11. Smith JM, Borgis S, Seifert V. Studies in urban ecology: The first wave of biological invasion by *Pistacia chinensis* in Armidale, New South Wales, Australia. *Aust Geogr Stud*. 2000;38(3):263-274.

    doi: 10.1111/1467-8470.00115

12. Hong-Lin L, Zhi-Xiang Z, Shan-Zhi L, Xiao-Xu L. Research advances in the study of *Pistacia chinensis* Bunge, a superior tree species for biomass energy. *For Stud China*. 2007;9:164-168.

    doi: 10.1007/s11632-007-0026-y

13. Liu JJ, Geng CA, Liu XK. A new pyrrolidone derivative from *Pistacia chinensis*. *Chin Chem Lett*. 2008;19(1):65-67.

    doi: 10.1016/j.cclet.2007.10.037

14. Koutsoudaki C, Krsek M, Rodger A. Chemical composition and antibacterial activity of the essential oil and the gum of *Pistacia lentiscus* Var. chia. *J Agric Food Chem*. 2005;53(20):7681-7685.

    doi: 10.1021/jf050639s

15. Özçelik B, Aslan M, Orhan I, Karaoglu T. Antibacterial, antifungal, and antiviral activities of the lipophylic extracts of *Pistacia vera*. *Microbiol Res*. 2005;160(2):159-164.

    doi: 10.1016/j.micres.2004.11.002

16. Mehenni C, Atmani-Kilani D, Dumarçay S, Perrin D, Gérardin P, Atmani D. Hepatoprotective and antidiabetic effects of *Pistacia lentiscus* leaf and fruit extracts. *J Food Drug Anal*. 2016;24(3):653-669.

    doi: 10.1016/j.jfda.2016.03.002

17. Nishimuta S, Taki M, Takaishi S, Iijima Y, Akiyama T. Structures of 4-aryl-coumarin (neoflavone) dimers isolated from *Pistacia chinensis* BUNGE and their estrogen-like activity. *Chem Pharm Bull (Tokyo)*. 2000;48(4):505-508.

    doi: 10.1248/cpb.48.505

18. Rashed K, Said A, Abdo A, Selim S. Antimicrobial activity and chemical composition of *Pistacia chinensis* Bunge

leaves. *Int Food Res J*. 2016;23(1):316.

19. Islam S, Hussain EA, Shujaat S, Khan MU, Ali Q. Antibacterial potential of propolis: Molecular docking, simulation and toxicity analysis. *AMB Express*. 2024;14(1):81.

    doi: 10.1186/s13568-024-01741-0

20. Ahmad R, Almubayedh H, Ahmad N, Naqvi AA, Riaz M. Ethnobotany, ethnopharmacology, phytochemistry, biological activities and toxicity of *Pistacia chinensis* subsp. integerrima: A comprehensive review. *Phytother Res*. 2020;34(11):2793-2819.

    doi: 10.1002/ptr.6720

21. Sana T, Zehra S, Khan M, *et al*. Urease and human glioblastoma (U87) cells growth inhibitory iridoid glycoside acetates from Nyctanthes arbor-tristis Linn. *Nat Prod Res*. 2024;6:1-9.

    doi: 10.1080/14786419.2024.2340059

22. Mishra A, Mulpuru V, Mishra N. An interaction network driven approach for identifying cervical, endometrial, vulvar carcinomic biomarkers and their multi-targeted inhibitory agents from few widely available medicinal plants. *Appl Biochem Biotechnol*. 2023;195(11):6893-6912.

    doi: 10.1007/s12010-023-04441-w

23. Akbar S, Das S. Synthesis, biological evaluation and molecular dynamics studies of oxadiazine derivatives as potential anti-hepatotoxic agents. *J Biomol Struct Dyn*. 2022;40(20):9974-9991.

    doi: 10.1080/07391102.2021.1938233

24. Maurya SK, Maurya AK, Mishra N, Siddique HR. Virtual screening, ADME/T, and binding free energy analysis of anti-viral, anti-protease, and anti-infectious compounds against NSP10/NSP16 methyltransferase and main protease of SARS CoV-2. *J Recept Signal Transduct Res*. 2020;40(6):605-612.

    doi: 10.1080/10799893.2020.1772298

25. Jia CY, Li JY, Hao GF, Yang GF. A drug-likeness toolbox facilitates ADMET study in drug discovery. *Drug Discov Today*. 2020;25(1):248-258.

    doi: 10.1016/j.drudis.2019.10.014

26. Lipinski CA, Lombardo F, Dominy BW, Feeney PJ. Experimental and computational approaches to estimate solubility and permeability in drug discovery and development settings. *Adv Drug Deliv Rev*. 2001;46(1-3):3-26.

    doi: 10.1016/s0169-409x(00)00129-0

27. Rudrapal M, Issahaku AR. *In silico* screening of phytopolyphenolics for the identification of bioactive compounds as novel protease inhibitors effective against SARS-CoV-2. *J Biomol Struct Dyn*. 2022;40(20):10437-10453.

    doi: 10.1080/07391102.2021.1944909

28. Wekesa EN, Kimani NM, Kituyi SN, Omosa LK, Santos CB. Therapeutic potential of the genus *Zanthoxylum* phytochemicals: A theoretical ADME/Tox analysis. *S Afr J Bot*. 2023;162:129-41.

    doi: 10.1016/j.sajb.2023.09.009

29. Silva AC, Borba JVV, Alves VM, *et al*. Novel computational models offer alternatives to animal testing for assessing eye irritation and corrosion potential of chemicals. *Artif Intell Life Sci*. 2021;1:100028.

    doi: 10.1016/j.ailsci.2021.100028

30. Raczyńska ED, Gal JF. Nitriles with high gas-phase basicity-part II transmission of the push-pull effect through methylenecyclopropene and cyclopropenimine scaffolds intercalated between different electron donor(s) and the cyano N-protonation site. *Molecules*. 2022;27(14):4370.

    doi: 10.3390/molecules27144370

31. Tsuneda T, Song JW, Suzuki S, Hirao K. On Koopmans' theorem in density functional theory. *J Chem Phys*. 2010;133(17):174101.

    doi: 10.1063/1.3491272

32. Huang CY, Chang YY, Chang ST, Chang HT. Xanthine oxidase inhibitory activity and chemical composition of *Pistacia chinensis* leaf essential oil. *Pharmaceutics*. 2022;14(10):1982.

    doi: 10.3390/pharmaceutics14101982

33. Abu-Izneid T, Rauf A, Akram Z, *et al*. Discovery of new α-glucosides, antiglycation agent, and *in silico* study of 2-(3, 4-dihydroxyphenyl)-7, 8-dihydroxy-3-methoxy-4H-chromen-4-one isolated from *Pistacia chinensis*. *Heliyon*. 2024;10(5):e27298.

    doi: 10.1016/j.heliyon.2024.e27298.

34. Noureen F, Khan MR, Shah NA, Khan RA, Naz K, Sattar S. *Pistacia chinensis*: Strong antioxidant and potent testicular toxicity amelioration agent. *Asian Pac J Trop Med*. 2017;10(4):380-389.

    doi: 10.1016/j.apjtm.2017.03.027

35. Bitew M, Desalegn T, Demissie TB, Belayneh A, Endale M, Eswaramoorthy R. Pharmacokinetics and drug-likeness of antidiabetic flavonoids: Molecular docking and DFT study. *PLoS One*. 2021;16(12):e0260853.

    doi: 10.1371/journal.pone.0260853

36. Parthiban A, Sachithanandam V. Isolation and biological evaluation 7-hydroxy flavone from *Avicennia officinalis* L: insights from extensive *in vitro*, DFT, molecular docking and molecular dynamics simulation studies. *J Biomol Struct Dyn*. 2023;41(7):2848-2860.

    doi: 10.1080/07391102.2022.2039771

37. Remila S, Atmani-Kilani D, Delemasure S, Connat JL, Azib L, Richard T, Atmani D. Antioxidant, cytoprotective, anti-inflammatory and anticancer activities of *Pistacia*

lentiscus (Anacardiaceae) leaf and fruit extracts. *Eur J Integr Med*. 2015;7(3):274-286.

doi: 10.1016/j.eujim.2015.03.009

38. Yemmen M, Landolsi A, Hamida JB, Mégraud F, Ayadi MT. Antioxidant activities, anticancer activity and polyphenolics profile, of leaf, fruit and stem extracts of *Pistacia lentiscus* from Tunisia. *Cell Mol Biol (Noisy-le-Grand)*. 2017;63(9):87-95.

doi: 10.14715/cmb/2017.63.9.16

39. Kermpatsou D. Study of the antiproliferative activity of the essential oil extracted from the plant *Pistacia lentiscus* var. *Chia Hum Cancer Cells*. 2021;06-29T07:43:20Z.

doi: 10.26257/heal.duth.11903

40. Pasban-Aliabadi H, Esmaeili-Mahani S, Najafipour H, Askari A, Jalalian H. Effects of baneh (*Pistacia atlantica*) gum on human breast cancer cell line (MCF-7) and its interaction with anticancer drug doxorubicin. *Iran J Pharm Res*. 2019;18(4):1959.

doi: 10.22037/ijpr.2019.1100853

41. Cháirez-Ramírez MH, De la Cruz-López KG, García-Carrancá A. Polyphenols as antitumor agents targeting key players in cancer-driving signaling pathways. *Front Pharmacol*. 2021;12:710304.

doi: 10.3389/fphar.2021.710304

42. Duan N, Hu X, Zhou R, Li Y, Wu W, Liu N. A review on dietary flavonoids as modulators of the tumor microenvironment. *Mol Nutr Food Res*. 2023;67(7):e2200435.

doi: 10.1002/mnfr.202200435

43. Suhail M, Tarique M, Tabrez S, Zughaibi TA, Rehan M. Synergistic inhibition of glioblastoma multiforme through an in-silico analysis of luteolin and ferulic acid derived from *Angelica sinensis* and *Cannabis sativa*: Advancements in computational therapeutics. *PLoS One*. 2023;18(11):e0293666.

doi: 10.1371/journal.pone.0293666

44. Abd Emoniem N, Mukhtar RM, Ghaboosh H, Elshamly EM, Mohamed MA, Elsaman T, Alzain AA. Turning down PI3K/AKT/mTOR signalling pathway by natural products: An *in silico* multi-target approach. *SAR QSAR Environ Res*. 2023;34(2):163-182.

doi: 10.1080/1062936X.2023.2181392

45. Ghosh A, Chakraborty D, Mukerjee N, *et al*. Target-based virtual screening and molecular interaction studies for lead identification of natural olive compounds against glioblastoma multiforme. *Environ Sci Pollut Res Int*. 2023;30(3):6170-6191.

doi: 10.1007/s11356-022-22401-5

46. Vibhavari RJA, Rao V, Cheruku SP, *et al*. Enhancing temozolomide antiglioma response by inhibiting O6-methylguanine-DNA methyltransferase with selected phytochemicals: *In silico* and *in vitro* approach. *3 Biotech*. 2023;13(12):385.

doi: 10.1007/s13205-023-03821-7

47. Mohamed GA, Abdallah HM. Unveiling the potential of phytochemicals to inhibit nuclear receptor binding SET domain protein 2 for cancer: Pharmacophore screening, molecular docking, ADME properties, and molecular dynamics simulation investigations. *PLoS One*. 2024;19(8):e0308913

doi: 10.1371/journal.pone.0308913

48. Siddique F, Daoui O, Ayoub M, *et al*. Identification and *in silico* screening of natural phloroglucinols as potential PI3Kα inhibitors: A computational approach for drug discovery. *Open Chem*. 2024;22(1):20240064.

doi: 10.1515/chem-2024-0064